EVALUATION OF MIXED MODE CRACK RESISTANCE CURVES USING BIAXIALLY LOADED SPECIMENS

C. Dalle Donne* and H. Döker*

Results obtained from biaxial load tests on cruciform specimens with inclined through thickness cracks and inclined cracks emanating from a hole are presented. It is shown that predominant mode II loading drives the stable crack in the direction almost parallel to the fatigue pre-crack. High (steel StE550) or moderate (Al2024-T3) mode I crack tip opening components causes a crack path deviation in the direction normal to the maximum tensile stress. The mixed mode crack resistance curves are presented in form of the magnitude of a crack tip displacement vector and compared with conventional R-curves of standard compact-tension (C(T)) and center-cracked-tension (M(T)) specimens. The effect of the load biaxiality is discussed with regard to previous experiments with mode I loaded cruciform specimens (1).

INTRODUCTION

In practical situations the loading experienced at a crack tip can be very complex resulting in mixed mode fracture. The question arises whether toughness values obtained from mode I loaded standard specimens are transferable to actual structures and whether the same restrictions apply to the transferability as in the mode I loading case (2). The objective of the present work was to study experimentally stable crack growth under mixed mode I and II loading in thin cruciform specimens and to compare the mixed mode R-curves to mode I R-curves of C(T) and M(T) specimens.

Several elastic-plastic finite element analyses (3,4) and experimental investigations (5,6) showed non uniform deformation and damage fields near an initially smooth notch tip under mixed mode I and II loading. One side of the notch, dominated by tensile stresses, blunts while the other side, dominated by shear strains, sharpens. Two competing fracture mechanisms occur at the sharpened and the blunted part of the notch respectively. Under predominant mode II loading a shear crack often initiates and propagates in the localised band of intense plastic strain (referred as "shear crack") (5,7,8). The highest tensile hydrostatic stress and notch tip con-

* German Aerospace Research Establishment DLR, Inst. of Materials Research, Cologne, Germany.

straint always occur near the blunted part of the notch (3,4). In this region crack initiation and propagation takes place due to microvoid coalescence. The crack growth direction is normal to the maximum tensile stress, i. e. the crack turns immediately upon initiation and experiences mode I loading ("tensile crack" growth). It dominates over a wide range of K_I/K_{II} ratios in high work hardening materials and in materials that fracture under small scale yielding (SSY) conditions (9,10,11).

In reference to the results of (4,12) the magnitude of a crack tip displacement vector $\delta_v = (\delta_I^2+\delta_{II}^2)^{0.5}$ is considered here as a candidate parameter for an unambiguous characterisation of material failure.

EXPERIMENTAL PROCEDURE

The cruciform specimens (Fig. 1) were machined form 5 mm thick sheets of a structural steel (StE550, Lüders yield strength $\sigma_Y = 580$ MPa, ultimate strength $\sigma_u = 650$ MPa) and from 6 mm thick sheets of an aluminum alloy (Al2024-T3, $\sigma_Y = 375$ MPa, $\sigma_u = 491$ MPa). The „cracked" cruciform specimen (Fig. 1a) contained a through thickness crack, whereas the „notched" cruciform specimen was distinguished by short cracks emanating from a hole (Fig. 1b). In both specimens the fatigue pre-cracks were inclined by an angle of 45° to the loading directions. The experiments were carried out on a biaxial test rig. The applied mixed ratio K_I/K_{II} was varied by changing the load biaxiality λ. A load ratio of -1 corresponded to pure mode II loading in both specimen types. In the cracked cruciform specimen K_I/K_{II} took the values of 0.31, 0.93 and 2.78 for the biaxiality ratios of -0.5, 0 (uniaxial) and +0.5 respectively. In the notched specimen uniaxial loading corresponded to $K_I/K_{II} = 1.73$.

The crack tip opening displacement was measured at the original fatigue crack tips with a specially designed clip-gage (1314). This gage allowed a decomposition of the measured displacements in the sliding and opening mode. In addition to visual observation through a microscope, the direct current potential drop method was used to monitor the amount of stable crack growth Δa during the tests. Further experimental details are given in (13).

RESULTS AND DISCUSSION

In Figure 2 the stable crack deflection angles α, measured on the broken specimens, are compared to the predicted directions normal to the maximum tangential stress and the maximum shear strain direction according to SSY plane stress (15) and plane strain (16) solutions. For both materials two types of macroscopic crack growth were observed. High mode II loading components ($\lambda < 0$) induced shear cracks which grew in a direction almost parallel to the pre-crack surface, even in the case of the Al2024-T3 specimens which fractured under contained yielding conditions. The shear fracture surfaces of the aluminum alloy specimens were smooth and featureless. In the near mode I ($\lambda \geq 0$) tested Al2024-T3 specimens a tensile crack initiated at the specimen midthickness and propagated as a straight

mode I crack in the direction perpendicular to the maximum tangential stress. In the ductile steel, which fractured under ligament yielding conditions, the stable crack extended in the maximum shear direction at much lower crack sliding components than in the aluminum alloy. Only high crack tip opening displacements ($\lambda = +0.5$) caused a crack path deviation in the direction normal to the maximum tensile stress. The constant offset between the predicted and measured shear deflection angles together with the dimples on the shear crack surfaces (13) of the steel specimens, suggests that the so called macroscopic „shear crack" in the steel specimens was in fact a combination of sliding off and void coalesce (17,18).

Figures 3 to 6 show the crack resistance curves of the cracked and the notched cruciform specimens in terms of the magnitude of the δ_5-clip displacement vector $\delta_{5,v} = (\delta_{5,I}^2+\delta_{5,II}^2)^{0.5}$ versus the amount of stable crack growth Δa. For comparison also the mode I δ_5- Δa curves of center cracked M(T) specimens (W = 125 mm, $a_0/W = 0.3$) and small C(T) specimens (W = 50 mm, $a_0/W = 0.6$) are plotted in the diagrams. The R-curves of the steel StE550 were virtually independent of mixed mode ratio and not influenced by the stress field of the notch (Fig. 3 and 4). Compared to the M(T) specimens lower fracture toughness in terms of $\delta_{5,v}$ were found. In case of shear crack growth this reduction was probably related to cracks progressing into the prestrained material of the shear band instead of the virgin material between the two shear bands of the symmetric (mode I) case (8). The crack tip opening displacement measured in the only steel experiment with a kinked crack ($\lambda = +0.5$) was reduced if compared with the M(T) results. This closing effect of tensile stresses parallel to the (kinked) crack became evident also in the mode I cruciform steel specimen tested at the same biaxial load ratio (1).

In the Al2024-T3 specimens biaxial loading with $\lambda \geq 0$ caused a crack deflection towards pure mode I opening. Like in the mode I tested cruciform specimen with $\lambda \geq 0$ (1) the crack resistance curves of the cracked specimen lie in the common scatterband of the standard C(T) and M(T) specimens (Fig. 5). High mode II loading components ($\lambda < 0$) drove the shear crack in its original direction and led to an apparent increase of fracture toughness. For a given Δa, the $\delta_{5,v}$ values were raised into the area of the δ_5-Δa curves of mode I cracked cruciform specimen tested at the same λ (1). In Figure 6 the $\delta_{5,v}$-Δa curves show virtually no effect of mixed-mode ratio, even if the two loading ratios showed two different crack propagation mechanisms (see Fig. 2). The higher resistance curves of the mixed-mode experiments compared to the mode I tests with notched cruciform specimen can be explained through the FEM analysis of Kfouri et al. (19). They demonstrated that the constraint conditions in the crack tip region decrease in severity as the pre-crack inclination angle increases.

CONCLUSIONS

Under predominant mode II loading, cracks due to shear type fracture grew in the maximum shear strain direction. High (case of steel) or moderate (case of alumi-

num alloy) mode I crack tip opening components caused a crack path deviation, i.e. the stable crack grew normal to the maximum tensile stress as a mode I crack. The R-curves in terms of the magnitude of the crack tip displacement vector $\delta_{5,v}$ of the StE550 steel were virtually independent of mixed mode ratio and not influenced by the stress field of a notch. In the aluminum alloy Al2024-T3 the toughness for shear crack growth (near mode II loading) was higher than that for tensile tearing (near mode I). The applied load biaxiality and the introduction of a notch affected the $\delta_{5,v}$ R-curves in a way similar to the mode I loaded cruciform specimens. Within the context of this work an estimation of crack resistance for biaxial loaded parts based on small C(T) specimens seems to be conservative for both materials.

The financial support by the Deutsche Forschungsgemeinschaft and the careful execution of the experiments by Mr. C. Sick are gratefully acknowledged.

REFERENCES

(1) Dalle Donne, C. and Döker, H., "Biaxial Load Effects on Plane Stress J-Δa- and δ_5-Δa-Curves", ECF 10, Schwalbe, K.-H. and Berger, C., Ed., EMAS, 1994, 891-900.
(2) Du, Z.Z., Betegón, C. and Hancock, J.W., Int. J. Fract., 52, 1991, 191-206.
(3) Aoki, S., Kishimoto, K., Yoshida, T. and Sakata, M., J. Mech. Phys. Solids, 35, 4, 1987, 431-455.
(4) Ghosal, A.K. and Narasimhan, R., J. Mech. Phys. Solids, 42, 6, 1994, 953-978.
(5) Otsuka, A., Thogo, K. and Okamoto, Y., Nucl. Engng. Design, 105, 1987, 121-129.
(6) Bhattacharjee, D. and Knott, J.F., Acta metall., 42, 5, 1994, 1747-1754.
(7) Davenport, J.C.W. and Smith, D.J., "Mixed-Mode Fracture of a Ferritic Steel", ECF 10, Schwalbe, K.-H. and Berger, C., Ed., EMAS, 1994, 901-910.
(8) Kardomateas, G. A. and McClintock, F.A., Int. J. of Fract., 35, 1987, 103-124.
(9) Hällback, N. and Nilsson, F., J. Mech. Phys. Solids, 42, 9, 1994, 1345-1374.
(10) Thogo, K. and Ishii, H., Engng. Fract. Mech., 41, 4, 1992, 529-540.
(11) Aoki, S., Kishimoto, K., Yoshida, T., Sakata, M. and Richard, H.A., J. Mech. Phys. Solids, 38, 2, 1990, 195-213.
(12) Saka, M. and Tanaka, S., Mech. of Mater., 5, 1986, 331-338.
(13) Dalle Donne, C. and Döker, H., „Plane Stress Crack Resistance Curves of an Inclined Crack Under Biaxial Loading", ASTM STP 1280, to appear 1997.
(14) Hellmann, D. and Schwalbe, K.-H., „Geometry and Size Effects on J-R and δ-R Curves under Plane Stress Conditions", ASTM STP 833, 1984, 577-605.
(15) Dong, P. and Pan, J., Engng. Fract. Mech., Vol. 37, No. 1, 1990, 43-57.
(16) Symington, M., Shih, C.F. and Ortiz, M., "Tables of Plane-Strain Mixed-Mode Plastic Crack Tip Fields", Report MRG/DMR-8714665/1, Brown University, Providence, R.I., U.S.A., 1988.
(17) Beachem, C.D., Metall. Trans. A, Vol. 6A, 1975, pp. 377-383.
(18) Kardomateas, G.A., McClintock, F.A. and Carter, W.T., Engng. Fract. Mech., 21, 2, 1985, 341-351.
(19) Kfouri, A.P., Wong, H.D. and Miller, K. J., Fatigue Fract. Engng. Mater. Struct.,15, 8, 1992, 743-762.

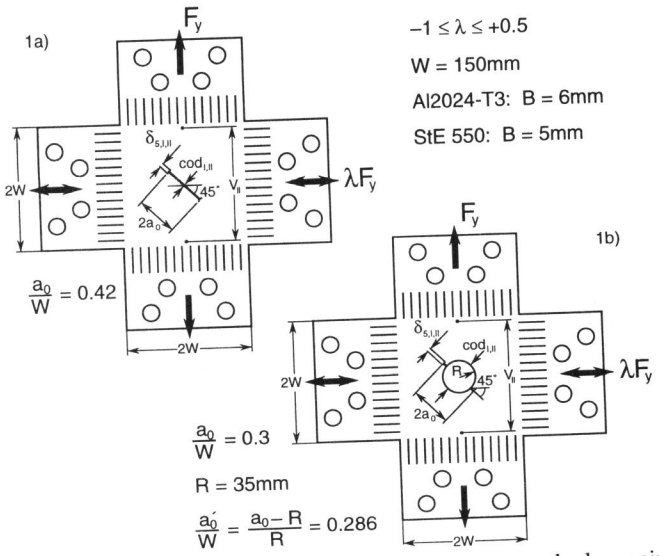

Fig. 1: Cruciform specimen with inclined cracks, 1a) „cracked specimen", 1b) „notched specimen".

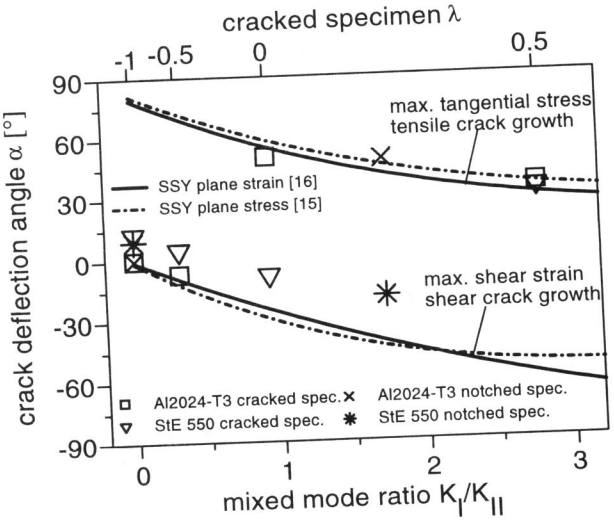

Fig. 2: Experimental crack deflection angles versus applied mixed mode ratio compared to plane stress and plane strain predictions.

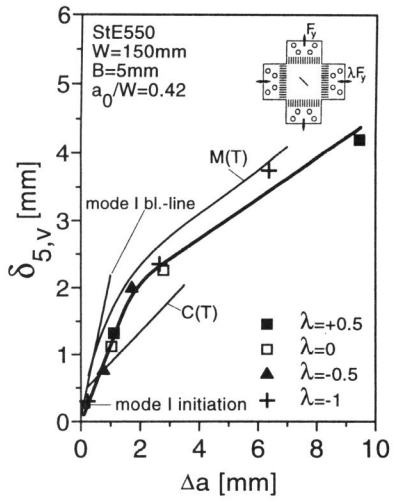

Fig. 3: R-curve of cracked steel specimen (multiple specimen method).

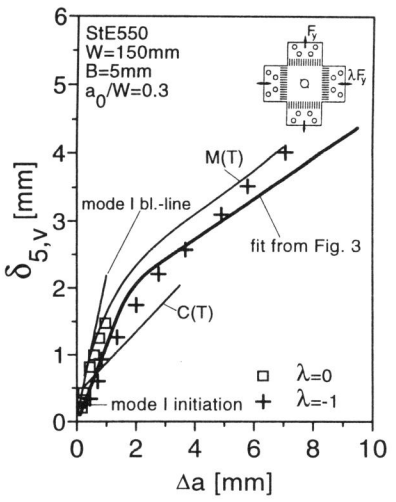

Fig. 4: R-curve of notched steel specimen (single specimen method).

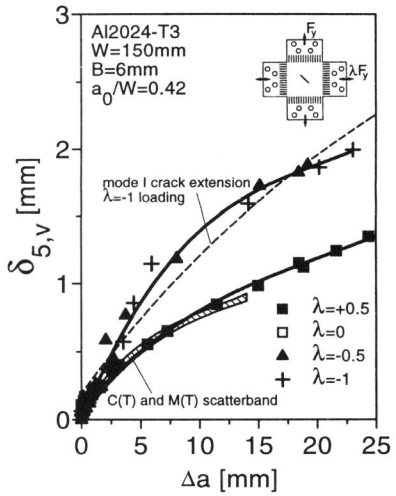

Fig. 5: R-curve of cracked Al-specimen (single specimen method).

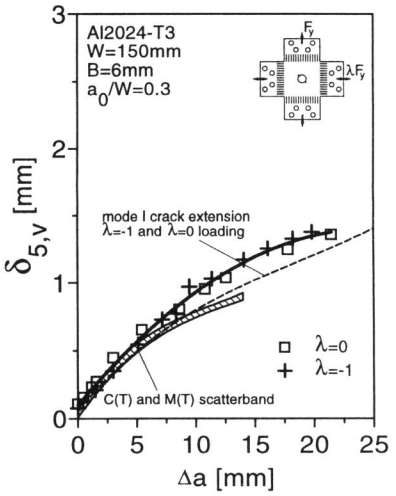

Fig. 6: R-curve of notched Al-specimen (single specimen method).